

# Soluble Expression and Purification of Biologically Active Human NANOG from *Escherichia coli*



Madhuri Thool, S. Sudhagar, and Rajkumar P. Thummer

**Keywords** NANOG · *E. coli* · BL21(DE3) · Recombinant protein · Secondary structure · Cancer · p27

## 1 Introduction

Homeobox (homeodomain) protein NANOG is a transcription factor of the ANTP (Antennapedia) class and is conserved in vertebrates [1, 2]. NANOG expression is observed during the initial stages of mouse embryonic development and in primordial germ cells [3–8]. During mouse embryonic development, lack of NANOG expression in the inner cell mass failed to produce epiblast, and instead, formed parietal endoderm-like cells [4]. Thus, the expression of NANOG is crucial for the epiblast formation [4, 9, 10]. Furthermore, the mRNA level of NANOG is downregulated after implantation [3]. High expression of NANOG holds epiblast essence, whereas low expression promotes differentiation into primitive endoderm. In embryonic stem cells (ESCs), NANOG is a vital player in the transcriptional pluripotency regulatory network along with OCT4 and SOX2 [11–13]. Moreover, the role of NANOG in ESCs is to maintain self-renewal and pluripotency in a cytokine-independent fashion [3, 4]. Intriguingly, the deletion of NANOG did not disrupt the chimera formation potential of ESCs [3].

---

M. Thool · R. P. Thummer (✉)

Laboratory for Stem Cell Engineering and Regenerative Medicine, Department of Biosciences and Bioengineering, Indian Institute of Technology Guwahati, Guwahati 781039, Assam, India  
e-mail: [rthu@iitg.ac.in](mailto:rthu@iitg.ac.in)

M. Thool · S. Sudhagar

Department of Biotechnology, National Institute of Pharmaceutical Education and Research Guwahati, Changsari, Guwahati 781101, Assam, India  
e-mail: [sudhagar.s@niperguwahati.ac.in](mailto:sudhagar.s@niperguwahati.ac.in)

Furthermore, ESCs are identical to induced pluripotent stem cells (iPSCs), and NANOG holds the potential for reprogramming due to the presence of the homeodomain, which is functionally preserved among all vertebrates [2]. The dose of NANOG is critical in cell-fusion-mediated reprogramming, and its overexpression improved the efficiency of reprogramming by 200-fold [14]. Several studies have reported that NANOG overexpression can enhance and hasten iPSC generation [9, 15]. Additionally, the role of NANOG in reprogramming is critical for reaching the pluripotent ground state by enabling the conversion of pre-induced pluripotent stem cells to bonafide iPSCs [9, 16]. Moreover, NANOG not only induces pluripotency but can also overcome reprogramming obstacles [17]. Inconsistent with these studies, a few studies have reported that including NANOG in the reprogramming cocktail does not improve reprogramming efficiency and is thus not critical for iPSC generation [18, 19]. Despite the deletion of the NANOG gene from somatic cells, these cells can be reprogrammed to form iPSCs and form teratomas and chimeras [19], indicating their dispensability in the reprogramming process. Another study reported that, although the elimination of NANOG decreased reprogramming efficiency, it was not required for iPSC generation [20]. Thus, these studies indicate that other members of the transcriptional network of pluripotency can substitute for NANOG loss. However, the same studies have suggested that NANOG is essential during the final stage of the reprogramming process and that its depletion affects reprogramming efficiency [19, 20]. Numerous reports have demonstrated the generation of human iPSCs using NANOG via lentiviral transduction [21–24]. In addition, the derivation of mouse and human iPSCs has also been reported using retroviral vectors, which include NANOG in the reprogramming cocktail [25, 26]. It is noteworthy that the use of viral-based approaches showed high reprogramming efficiency but induces genomic alteration. To circumvent these limitations of including viral components, several other approaches, such as recombinant proteins, mRNA, Sendai virus and miRNAs, are favored [27, 28]. Among all the approaches for iPSC generation, the recombinant protein-based method is the safest [29].

Recombinant proteins are of great importance for industrial applications and clinical research. The benefits of using bacterial systems, such as *Escherichia coli* (*E. coli*), for the production of recombinant proteins are easy genetic manipulation and low production costs. However, this system also has several unavoidable blockages, such as codon usage bias, weak expression, insoluble expression, complicated purification protocols, protein misfolding and so forth. Thus, the expression of recombinant proteins opens an avenue for the generation of iPSCs. These cells can serve as patient-specific cells for cell therapies. Herein, the generation of a recombinant human NANOG fusion protein along with its secondary structure determination is reported, which possesses cytoplasmic and nuclear translocation ability, and is demonstrated to be biologically active. This recombinant version of human NANOG can potentially be used in the cocktail of transcription factors for iPSC generation.

In addition to the role of NANOG in iPSCs generation, anomalous NANOG expression has been shown in different types of human malignancies. Furthermore, ectopic expression of NANOG caused augmented proliferation and downregulation of tumor suppressors, however, it did not result in tumor formation. Therefore, unlike

other reprogramming factors, NANOG cannot be considered an oncogene [30]. In stark contrast to earlier finding, several studies have reported NANOG expression in different tissues, including the breast, cervix and kidney [31–33]. Several such studies will provide a deeper understanding of molecular networks in cancer and help in prognosis and treatment. Thus, the recombinant version of human NANOG generated in this study can further be helpful to understand the biological role of NANOG in cancer.

## 2 Materials and Methods

### 2.1 Plasmids, Strains, Reagents and Cell Lines

The personalized plasmids (pUC-HTN-*GOI* and pUC-*GOI*-NTH) were procured from GenScript. *E. coli* BL21 (DE3) cells were utilized as host for recombinant protein expression. Isopropyl  $\beta$ -D-1-thiogalactopyranoside (IPTG), Luria–Bertani broth, terrific broth, kanamycin, sodium phosphate mono/dibasic, sodium chloride and imidazole was purchased from HiMedia. Bradford reagent was purchased from Bio-Rad. Dulbecco’s Modified Eagle medium (DMEM), fetal bovine serum (FBS) and penicillin–streptomycin solution (P/S) were purchased from Invitrogen.

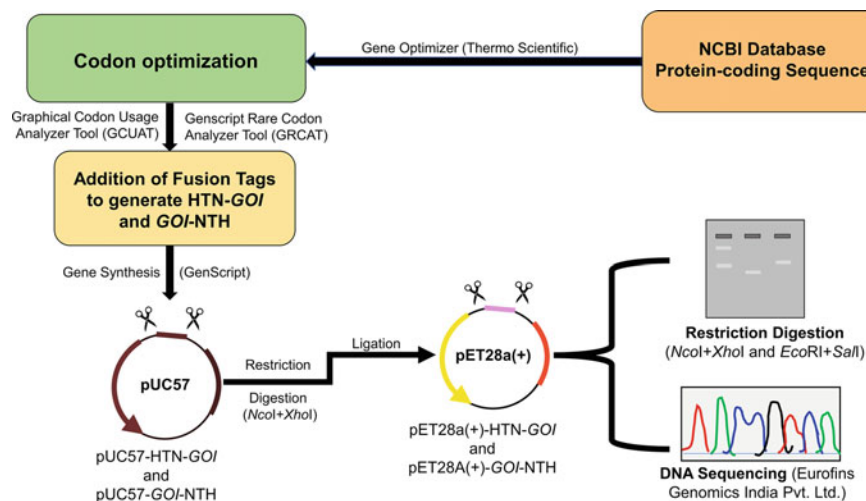
Apart from this, two human cell lines, HeLa (NCCS, India) and human dermal fibroblasts [HDFs; HiMedia CL011-2XT25], were cultured in a complete growth medium [DMEM, FBS (5%) and P/S (1%)].

### 2.2 Construction of Expression Vector and Optimization for Soluble NANOG Expression

A schematic figure detailing the stepwise process from retrieval of gene sequence [codon-optimized coding sequence of *NANOG* along with a set of fusion tags (Table 1) (gene inserts)] to cloning to confirmation of cloning of *NANOG* in desired vector is shown in Fig. 1. Furthermore, pET28a(+)-HTN-*NANOG* and pET28a(+)-*NANOG*-NTH were transformed into BL21(DE3) cells using  $\text{CaCl}_2$  method. To identify the optimal expression, the same approach was used as designated earlier [34, 35]. The cells were lysed using the lysis buffer mentioned in Table 2.

**Table 1** Fusion tags used in the study

Fusion tags	DNA sequence (5'-3')	Protein sequence
His (H)	CATCATCACCACCATCACCATCAT	HHHHHHHHH
TAT (T)	GGTCGTAAAAAACGTCGTCAGCGTCGTCGCCCT	GRKKRRQRRRPP
NLS (N)	AAAAAAAAGCGCAAAGTG	KKKRKV

**Fig. 1** Diagram representation of the codon optimization and cloning strategy used in this study. H, Histidine; T, TAT, Trans-activator of transcription; N, NLS, Nuclear localization sequence/signal**Table 2** List of buffers and their composition used for the purification

Ingredients	Lysis buffer	Wash buffer 1	Wash buffer 2	Wash buffer 3	Elution buffer
Phosphate buffer (mM)	20	20	20	20	20
Sodium chloride (mM)	150	150	150	150	150
Imidazole (mM)	20	50	100	200	500
pH (room temperature)	7.8	7.8	7.8	7.8	7.8

### 2.3 One-Step Purification of NANOG Via Metal Affinity Chromatography

To purify HTN-NANOG fusion protein, 1.2 L of lysate of the recombinant *E. coli* BL21(DE3) cells harboring pET28a(+)-HTN-NANOG were established as

mentioned above. The resulting lysate was loaded onto the pre-equilibrated nickel-NTA column, followed by complete washing with buffers and then eluted with elution buffer. The composition of all buffers for purification purpose is mentioned in Table 2.

After purification, size-exclusion chromatography of the eluted fractions was performed as previously described [34]. The collected protein fractions were quantified using the Bradford assay [36].

## ***2.4 SDS-PAGE, Coomassie Staining and Western Blotting (Immunoblotting) Analysis***

SDS-PAGE, Coomassie staining and Western blotting (immunoblotting) was performed as previously described [35]. The primary antibodies [anti-His (BioBharati, BB-AB0010; 1:5000), anti-NANOG (Merck Millipore, AB9220; 1:5000)], anti-GAPDH (BioBharati, BB-AB0060; 1:5000), anti-H3 (BioBharati, BB-AB0055; 1:5000), anti-p27 (Cell Signaling Technology, D69C12; 1:4000),  $\beta$ -actin (BioBharati, BB-AB0024; 1:5000), and secondary antibodies [anti-rabbit IgG antibody (Invitrogen, 31,460; 1:5000)] were used in the immunoblot analysis.

## ***2.5 Circular Dichroism (CD) Spectroscopy***

The full-length HTN-NANOG protein secondary structure was determined by CD spectroscopy [J-1500 spectropolarimeter (Jasco, MD, USA)] and further scrutinized by online tool BeStSel (Beta Structure Selection) [37, 38] as previously described [34, 35].

## ***2.6 Stability of HTN-NANOG Protein***

Stability was performed as described previously [39] and clarified samples were then evaluated by immunoblotting using the NANOG antibody.

## ***2.7 Subcellular Fractionation***

HDFs cells ( $1 \times 10^5$ ) were seeded in a T-25 flask and incubated overnight with vehicle control or HTN-NANOG protein (400 nM). Subcellular fractionation was carried

out as previously described [40] and analyzed by immunoblotting with specific antibodies.

## **2.8 Cell Proliferation Assay**

HDFs ( $1 \times 10^4$  cells/well) were seeded in 24-well plates and were treated with HTN-NANOG (200 nM) or vehicle control. After reaching approximately 70–80% confluency, the cells were trypsinized. Cell counting was performed using a hemocytometer [41]. A cell suspension was intermixed with exclusion dye solution (Bio-Rad) and loaded into the cell counting chamber. Later, the live cells within a specific area were counted and recorded. Because the chamber volume is well-defined (commonly  $0.1 \text{ mm}^3$ ), the number of cells calculated per area multiplied by the dilution factor determines the number of live cells per mL. The data are presented with a graph of the cumulative cell number against days.

## **2.9 Cell Migration (Scratch) Assay**

HeLa cells ( $0.6 \times 10^5$ ) were seeded in a 24-well plate in a growth medium. Scratch assay was performed as earlier [42]. The rate of cell migration was calculated as previously described [43].

## **2.10 RT-qPCR Analysis**

HeLa cells ( $1 \times 10^5$  cells per well) were seeded in a six-well plate and treated with vehicle control or HTN-NANOG protein (200 nM) for 3 consecutive days. RNA isolation, synthesis of complementary DNA and RT-qPCR were performed and analyzed as described previously [44]. The primers used in this study are mentioned in Table 3.

## **2.11 Statistical Analysis**

Data analysis (unpaired student's t-test) were analyzed using GraphPad Prism 8 software and presented as mean  $\pm$  standard deviation (SD) of three independent experiments. Values of  $p < 0.05$  (\* $p < 0.05$ ; \*\*\* $p < 0.001$ ) were with statistical significance.

**Table 3** Primers used in this study

Gene	Primer sequence (5'–3')	Annealing temperature (°C)	Product size (bp)
GAPDH	Reverse: ACCACCCTGTTGCTGTAGCCAA	58	131
	Forward: GTCTCCTCTGACTTCAACAGCCAA		
<i>p<sup>27</sup></i>	Reverse: CAAGCACCTCGGATTTT	52.6	101
	Forward: CTGCCCTCCCCAGTCTCTCT		

### 3 Results

#### 3.1 Cloning and Expression Parameter Optimization

The coding (codon-optimized) sequence of human *NANOG* was fused with three fusion tags as shown in Table 1, Fig. 1. The fused gene insert was cloned in pET28a(+) to generate two constructs as shown in Fig. 1. These genetic constructs were verified using restriction analysis using enzymes (Fig. 2) and DNA sequencing. These genetic constructs were transformed in *E. coli* strain BL21(DE3) for expression. Next, expression parameters were identified by screening different values (Table 4) for maximal soluble expression.

Based on these observations, maximal soluble expression of NANOG fusion proteins was observed with the gene constructs (HTN-NANOG and NANOG-NTH) induced at 18 °C (Fig. 3). However, no soluble expression of HTN-NANOG was

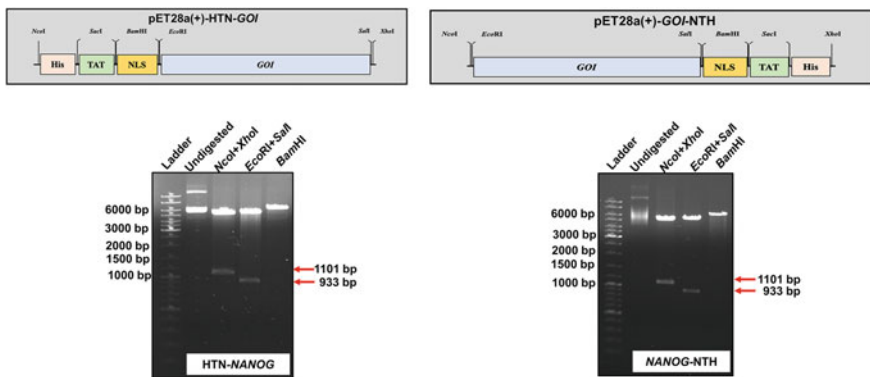


**Fig. 2** Cloning of gene inserts, HTN-NANOG and NANOG-NTH, in pET28a(+) expression vector. The *GOI* was fused as per the schematic diagram (top) with human *NANOG* cDNA sequence to generate pET28a(+)-HTN-NANOG and pET28a(+)-NANOG-NTH. The resulting plasmids were then confirmed by restriction digestion using various restriction enzymes. *GOI*, *Gene of interest*; H, His; T, TAT and N, NLS

**Table 4** Summary of the optimal expression conditions to obtain maximal expression of the human HTN-NANOG fusion protein in *E. coli*

Expression parameters	Values screened	Optimal value
Inducer concentration (IPTG) (in mM)	0.05, 0.1, 0.25, 0.50	0.1
Induction cell density (OD <sub>600</sub> )	~0.5, ~1.0, ~1.5	~0.5
Post-induction incubation time (in hours)	2, 4, 8, 12	12
Induction temperature (in °C)	18, 37	18

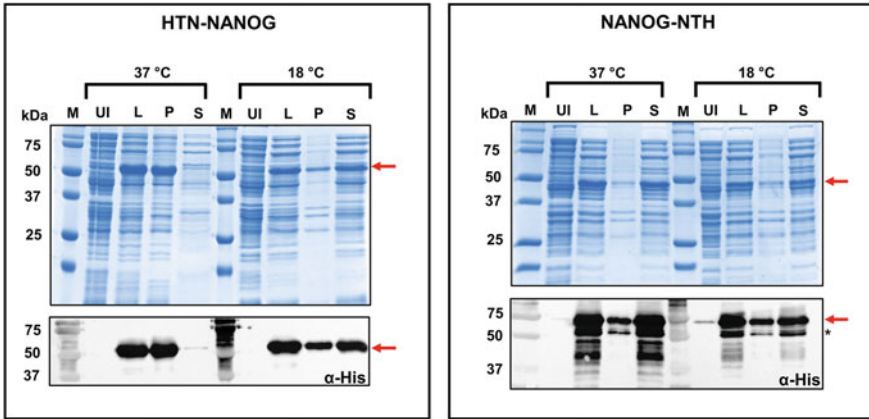
induced at 37 °C, and many truncations were observed for NANOG-NTH (37 °C) (Fig. 3). Hence, these constructs were excluded from further analyses. Notably, in the case of NANOG, only N-terminally tagged NANOG (HTN-NANOG) induced at 18 °C showed the maximal soluble expression with no truncations. Hence, this gene construct (HTN-NANOG), induced at 18 °C with a post-induction incubation time of 12 h, was selected for further experiments (Fig. 3). These results demonstrate that the solubility of the protein was improved by reducing the temperature of the induced culture. Several studies have demonstrated the expression and purification of full-length and truncated recombinant NANOG proteins from several mammalian species [12, 45–51]. However, these studies only showed the interaction of NANOG with its consensus DNA binding sequence [12, 45, 49–51], however, the comprehensive demonstration of bioactivity of full-length human NANOG is still obscure. Thus, this study mainly focuses on the exploration of the bioactivity of full-length recombinant NANOG protein.

### 3.2 Purification and Secondary Structure Estimation of HTN-NANOG Protein

After screening the parameters for soluble expression analysis, HTN-NANOG was expressed in soluble form when induced at 18 °C. Hence, we aimed to purify this protein using a simple and straightforward affinity chromatography-based purification procedure. The HTN-NANOG protein band (~55 kDa) was observed in the elution fractions (Fig. 4). The purified HTN-NANOG protein was identified using SDS-PAGE (Fig. 4; top) and immunoblotting using a histidine antibody (Fig. 4; middle) and NANOG antibody (Fig. 4; bottom). Both antibodies detected all protein fragments, proving that there was no bacterial protein. Thus, we have demonstrated simple and straightforward native purification of the NANOG fusion protein.

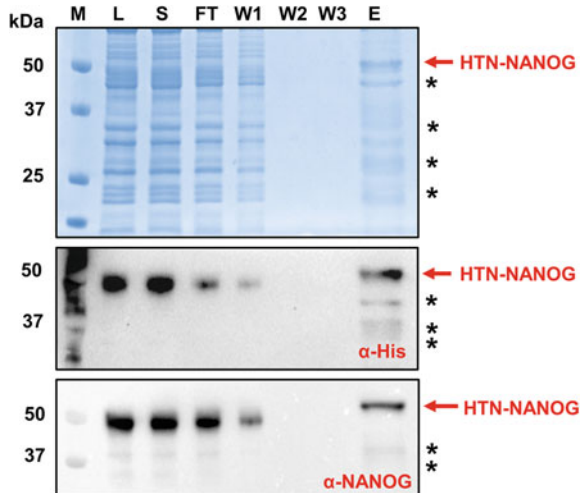
The far-ultraviolet CD spectroscopic method is widely used to unveil the folding features of certain proteins where the secondary structure is obscure [52, 53]. Thus,





**Fig. 3 Identification of the optimal induction temperature to achieve maximal soluble expression of recombinant human NANOG fusion protein.** *E. coli* BL21(DE3) strain was transformed with pET28a(+) vectors harboring the fusion gene inserts and the expression of both N-terminally tagged and C-terminally tagged recombinant NANOG protein was at two different temperatures: 37 °C (post-incubation time of 2 h) and 18 °C (post-incubation time of 12 h). Then, the harvested cells were lysed to obtain the total cell lysate (L) fraction and further centrifuged to obtain a soluble/supernatant (S) cell fraction and an insoluble/pellet (P). Protein samples (20 μg) were loaded on 12% SDS-PAGE gel and further verified by immunoblotting (bottom). M, Marker; UI, uninduced (total cell lysate); L, cell lysate; P, pellet portion; S, supernatant portion; kDa, kilodaltons; α, antibody. (n = 4) \* Truncation of fusion proteins

**Fig. 4 SDS-PAGE and immunoblot analysis of NANOG fusion protein purification by metal affinity chromatography.** HTN-NANOG protein. M, Marker; L, Lysate; S, Supernatant portion; FT, Flow-through portion; W (1-3), Wash buffer (1-3); E, Elution portion; kDa, Kilodalton; α, Antibody



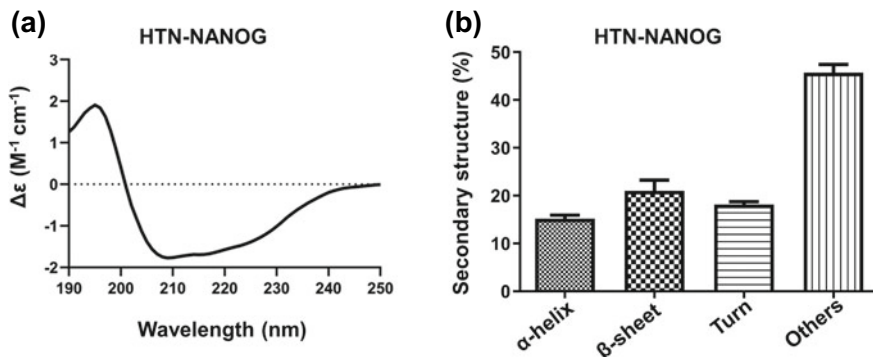


**Fig. 5 Determination of the secondary structure of the NANOG protein using far-UV CD spectroscopy.** The purified NANOG protein was analyzed for its secondary structures using far-UV CD spectroscopy. **a** The CD spectra were represented as delta epsilon ( $M^{-1} cm^{-1}$ ; Y-axis) vs wavelength (nm; X-axis). **b** CD spectra were evaluated with the BeStSel online tool, and the resulting structural configuration ( $\alpha$ -helix,  $\beta$ -sheets, turn and others) is represented using bar graphs ( $n = 3$ )

the secondary structural conformation of purified recombinant HTN-NANOG was evaluated using CD (Fig. 5a). CD spectrum analysis using the BeStSel tool suggested that this fusion protein consisted primarily of random coils (~46%), followed by  $\beta$ -sheets (~21%), turns (~18%) and  $\alpha$ -helices (~15%) (Fig. 5b). The results account that purified recombinant HTN-NANOG protein has a secondary structure retained post-purification.

### 3.3 Stability and Transduction Ability of HTN-NANOG Fusion Protein

Further, the protein stability of the purified NANOG protein was studied. This fusion protein was found to be stable for at least 24 h, which was identified using immunoblotting with the NANOG antibody (Fig. 6a, b).

Next, we demonstrated the transduction ability of HTN-NANOG fusion protein in HDFs using subcellular fractionation. HDFs have no endogenous expression of NANOG; therefore, these cells were used in this study. Similar to immunofluorescence staining, subcellular fractionation can also be used to know the protein localization in a cell [40, 54]. Moreover, subcellular localization is vital for proper protein function. The fractions (nuclear and cytoplasmic) of the human cell lines were separated by centrifugation. These fractions were further analyzed by immunoblotting. In this study, GAPDH (Glyceraldehyde-3-Phosphate Dehydrogenase) and Histone H3 were used as internal loading controls for the cytoplasmic (GAPDH) and nuclear (H3) fractions (Fig. 6c), respectively. Immunoblotting analysis exhibited that the majority of the HTN-NANOG fusion proteins were present in the nuclear fraction

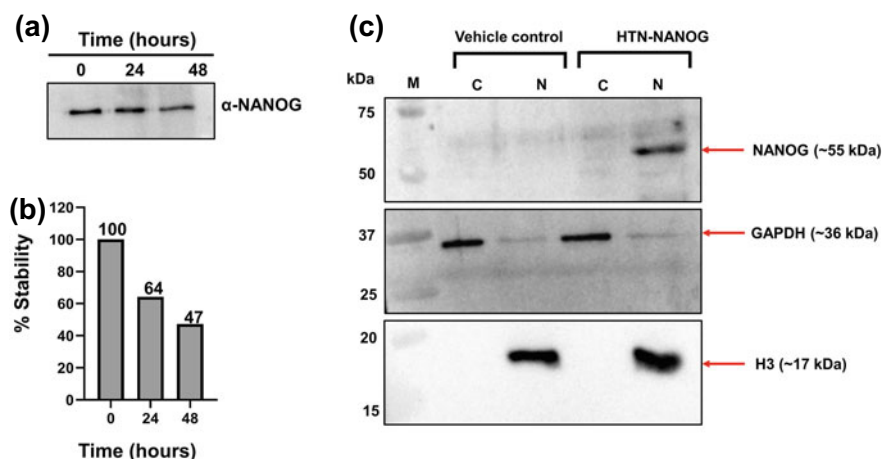


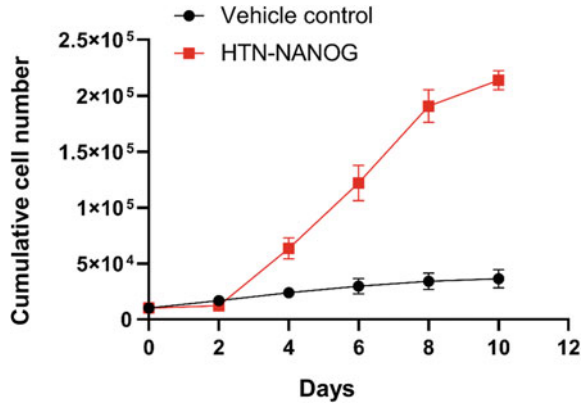
**Fig. 6** Stability and localization of HTN-NANOG protein determined with a subcellular fractionation assay. **a** Stability of purified recombinant proteins under standard cell culture conditions was analyzed by immunoblotting. **b** Densitometric analysis of data from (a) and (c) representative immunoblot showing cytoplasmic (C) and nuclear (N) fractions of NANOG fusion protein-treated or untreated (vehicle control) HDFs cells using NANOG, GAPDH and Histone H3 antibodies. M, Marker; C, Cytosolic portion; N, Nuclear portion

of cells treated with NANOG. This implied that the fusion tag nuclear localization signal (NLS) is responsible for the efficient nuclear translocation of the recombinant fusion protein. The homeodomain in human NANOG tends to be localized in the nucleus, implying that it has a NLS [55]. The presence of a stretch of six amino acids [YKQVKT (136–141 aa)] in the homeobox is responsible for nuclear localization [56]. Adding an extra NLS to NANOG sequence has further enabled efficient nuclear delivery of the purified recombinant NANOG protein.

### 3.4 Effect of the Recombinant HTN-NANOG Protein on Cell Proliferation of HDFs

Several studies have reported that exogenous expression of NANOG in ESCs and fibroblasts resulted in increased cell proliferation [57, 58]. In view of this, we also explored the effect of NANOG on human fibroblast (HDF) cells. To investigate cell proliferation, we counted the cells using a hemocytometer at different time intervals and observed augmented cell proliferation of HDFs. The data was analyzed and are shown in Fig. 7. The results of our study are in concordant with prior studies [57, 58]. Hence, our study provides evidence that NANOG plays a proliferative role in HDFs and is bioactive.

**Fig. 7 Effect of purified HTN-NANOG protein on cell proliferation.** Cell proliferation was assessed via cell counting. Y-axis signifies the cumulative cell number, and the X-axis signifies days of treatment (n = 3)



### 3.5 Effect of the Recombinant HTN-NANOG Protein on the Migration of HeLa Cells

The oncogenic potential of NANOG is well established and its presence has been detected in cervical cancer [33, 59, 60]. Forced NANOG expression has been reported to result in increased migration, invasion and tumorigenesis in HeLa cells [61]. Thus, to confirm that the purified HTN-NANOG fusion protein was biologically active, the migration rate of HeLa cells was evaluated using an in vitro scratch assay. Based on the observation of the effect of HTN-NANOG protein transduction in HeLa cells, NANOG protein-treated wells showed faster cell migration compared to the wells treated with the vehicle control (Fig. 8a, b; \*\*\* $p < 0.001$ ). These results were consistent with previously published results [61]. An earlier study used NANOG mRNA, but we used NANOG as a recombinant protein in our study for functional investigation. Thus, this study demonstrated that the HTN-NANOG fusion protein facilitated the migration of HeLa cells and was bioactive.

### 3.6 Effect of the Recombinant HTN-NANOG Protein on the Cell Cycle Inhibitor P27 Gene

To further explore the functional characteristics of NANOG, we investigated the effect of NANOG on cell cycle factor p27 (CDKN1B). Furthermore, p27<sup>Kip1</sup> is a tumor suppressor and inhibitor of Cyclin/Cyclin-Dependent Kinase (CDK) complexes. Thus, p27 plays a vital role in the regulation of the cell cycle. Transient activation of NANOG in fibroblasts is linked to the downregulation of p27 [62]. Hence, we also attempted to examine the effect of HTN-NANOG on p27 mRNA and protein levels in HeLa cells. Cells were harvested for RNA isolation and complementary DNA (cDNA) synthesis was carried out from total RNA. Quantitative real-time

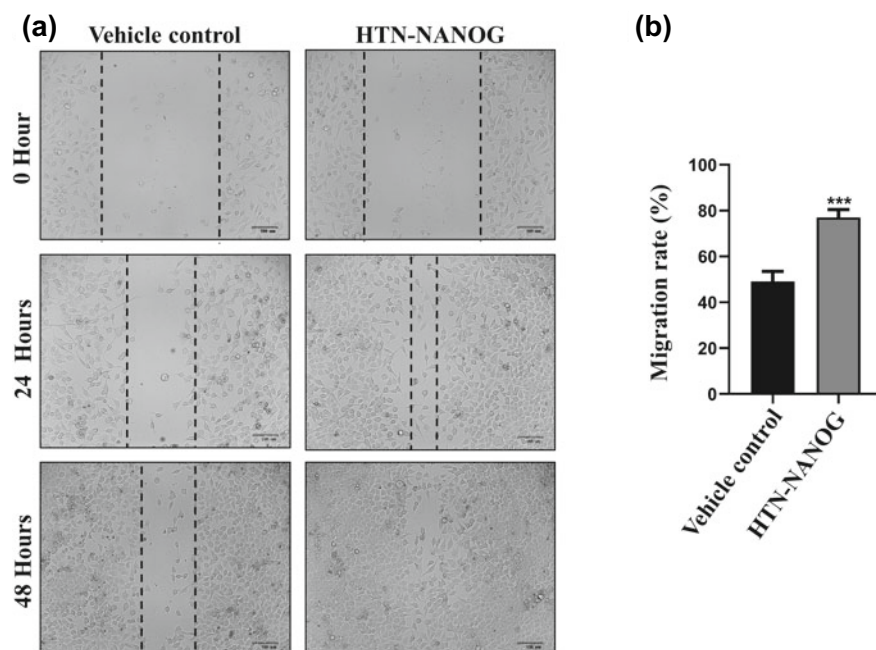


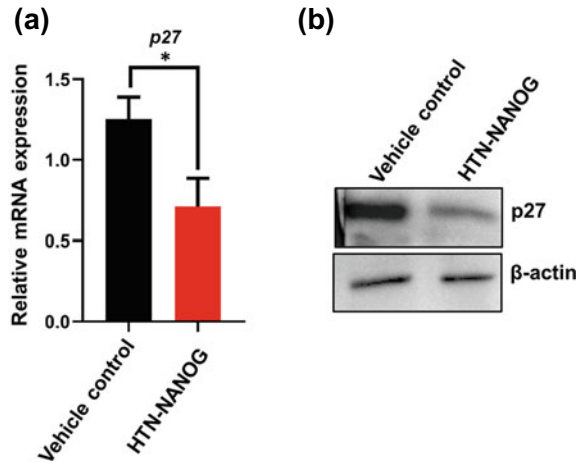
**Fig. 8** Effect of purified HTN-NANOG protein on the migration of HeLa cells. **a** Scratch assay of HeLa cells. Cell migration was induced in the presence of HTN-NANOG. Scale bar: 100  $\mu$ m. **b** Graphical representation of the changes in migration rate following treatment with vehicle control or NANOG protein. Quantitative data are expressed as the mean  $\pm$  SD (n = 3). \*\*\*p < 0.0001

PCR (RT-qPCR) was performed using GAPDH as a reference. The data indicated a significant decrease in the p27 at RNA level (Fig. 9a; \*p < 0.05). To further validate this at the protein level, we performed immunoblotting using  $\beta$ -actin as a loading control for normalization (Fig. 9b). Immunoblotting analysis showed that the expression of p27 was downregulated at the protein level in the presence of HTN-NANOG. These data demonstrate that the downregulation of the p27 (at RNA and protein level) in the presence of protein is in line with an earlier reported study [62]. Hence, this confirms that the purified recombinant HTN-NANOG protein is bioactive.

## 4 Discussion

Human NANOG (915 bp) contains four exons and three introns. The human NANOG protein is a long chain of 305 amino acids and has N-terminal, homeobox domain and C-terminal region. The N-terminal region (94 aa) is abundant in serine, proline and threonine and is responsible for governing the transcription of NANOG. The homeobox domain (60 aa) binds to the DNA core region. The C-terminal region (151 aa)

**Fig. 9 Effect of the purified HTN-NANOG fusion protein on p27 levels in HeLa cells.** **a** Relative expression of the p27 mRNA in vehicle control and HTN-NANOG analyzed by RT-qPCR. Quantitative statistics are shown as the mean  $\pm$  SD (n = 3). \*p < 0.05. **b** Immunoblot analysis of p27 protein expression in the presence of the vehicle control and NANOG protein (n = 3)



is tryptophan-rich, and investigations have shown that this region is responsible for homodimerization. Thus, NANOG acts as a transcription factor by controlling transcription through interactions with the promoters of myriad genes via these domains [55, 56, 63]. NANOG is a transcriptional activator that binds to the 5'-TAAT-3' essential regions of the DNA sequence [64, 65]. A triad of transcription factors, including OCT4, SOX2 and NANOG, appear to be at the heart of pluripotency [11]. Unlike OCT4 and SOX2, solitary NANOG cells conserve pluripotency in the absence of pluripotency maintenance signals. Knockdown studies have revealed the crucial role of NANOG in embryogenesis staging. NANOG is important for the maintenance of self-renewal and pluripotency. These properties prevent the ESCs and iPSCs from differentiation [11].

Additionally, NANOG facilitates pre-iPS cells to attain ground-state pluripotency (iPSCs), which is crucial in the process of molecular reprogramming [9]. During the reprogramming of somatic cells, NANOG plays a critical role in inducing pluripotency [9]. NANOG boosts the activation of STAT3; hence, the synergistic action between them promotes the establishment of naive pluripotency in ESCs and during the initial stages of reprogramming [66]. iPSCs that are deficient in NANOG are identical to wild-type iPSCs in transcriptional status; and upon further exploration, teratomas and chimeric formation are underpinned. Hence, this study demonstrates that NANOG is dispensable for iPSC formation [19]. A recent study has demonstrated the distinctive ability of human NANOG to initiate prion-like clusters. These assemblies could act as a means for delivering DNA elements for their interactions with others, which is essential for the re-organization of chromatin structures and activation of ground-state pluripotency in a dose-dependent manner [67].

We successfully purified HTN-NANOG from a soluble fraction of *E. coli* cultures using affinity chromatography. Based on these observations, the soluble protein expression was relatively low (purity >90%) and might be due to its aggregation property when induced at larger volumes. Additionally, another study reported the

purification of human NANOG, in which, among all the domains, the C-terminal domain has limited solubility. In contrast, the homeodomain and N-terminal domains are favorably soluble [51]. Strikingly, another study also showed the expression of full-length human NANOG protein along with 17 kDa protein (Skp) chaperone [51]. The role of Skp is to aid the folding of outer membrane proteins and their entry into membranes. Furthermore, Skp is well established to enhance the folding of recombinant proteins and further, directs the cargo to the periplasm of *E. coli* [68]. In agreement with the preceding evidence, the wild-type NANOG-GB1 fusion protein was also expressed and found to be soluble when co-expressed with the Skp chaperone. This study reasoned that the Skp chaperone is equipped with a hydrophobic cage that encases wild-type NANOG and further co-operates with tryptophan residues upon exposure [67]. In addition, human NANOG, by virtue of its C-terminal domain, is apt for aggregation, which accounts for the limited biophysical characterization of the protein and its individual domains [67]. Therefore, we aimed to determine the secondary structure of the full-length NANOG fusion protein.

The crystal structure of homeodomain NANOG has been documented as a structural scaffold formed by three helices in both mice and humans [45, 69]. A recent study showed that the CD spectra of each domain individually, the N-terminal domain of human NANOG, comprises intrinsically disordered regions responsible for displaying a random-coil signature in NMR spectra and are further found in line with the computational prediction [67]. In contrast, the far-UV CD spectra of the C-terminal domain revealed  $\beta$ -sheets and resulted in a reduced number of  $\beta$ -sheets in the mutated version of human NANOG [67]. According to available data, our study showed that the secondary structure of the full-length HTN-NANOG protein is retained and is likely to be bioactive.

A multitude of studies has been reported on the generation of reprogramming factors, namely, OCT4, SOX2, NANOG, PDX1, NGN3, GLIS1, GATA4, TBX5, HAND2, ETS2, MEF2C and MESP1, in *E. coli* using similar approaches [35, 40, 42, 44, 58, 62, 70–78]. These investigations also revealed the utility of NLS in proteins that facilitate the delivery of recombinant proteins to the nucleus in human cells. Several reports have observed that the fusion tags [post protein delivery into cells (via TAT) and their nucleus (via NLS)] do not hamper the bioactivity of recombinant proteins [35, 39, 40, 44, 58, 62, 70–73, 78]. Thus, cytoplasmic and nuclear transport of reprogramming factors can be attained via TAT and NLS fusion without requiring additional transduction reagents. For this, we demonstrated that the protein is stable under standard cell culture conditions and has the ability to enter the nucleus using a subnuclear fractionation assay.

Additionally, our study highlights the proliferative effect of recombinant NANOG on human dermal fibroblasts, emphasizing its role in malignancy. Next, we analyzed the impact of exogenously delivered NANOG fusion proteins on HeLa cell migration. Thus, we revealed that the stem cell-linked factor NANOG possesses tumorigenic properties in cervical cancer. Furthermore, we observed the downregulation of p27 in HeLa cells in the presence of NANOG at the mRNA and protein levels. This study provides evidence that tagging the protein at either terminal does not hinder its bioactivity. The generation of biologically active NANOG might trigger the endogenous

expression of NANOG and may also participate in the auto- and inter-regulatory loops of pluripotency during the induction of iPSCs. The proliferative effect of NANOG on cells may offer an excellent platform for the expansion of mature cells in vitro. From a cancer perspective, it may act as a molecular marker for prognosis and cure.

**Acknowledgements** North Eastern Region—Biotechnology Programme Management Cell (BT/PR16655/NER/95/132/2015), DBT, Govt. of India funded this study.

**Author Contribution** MT designed and performed the experiments, assembled and analyzed the data, wrote the manuscript; SS analyzed and interpreted the data; and RPT conceptualized and designed the study, analyzed the data, supervised the experiments, wrote the manuscript, and provided financial support. The final draft of the manuscript was approved by all the authors for publication.

**Declarations** None.

**Conclusion** The purification of HTN-NANOG fusion protein from *E. coli* with a retained secondary structure and its bioactivity in human cells is demonstrated in this study. This study reported that human NANOG fusion protein enhanced proliferation, migration and downregulated p27 gene expression in HeLa cells, demonstrating its bioactivity. This biologically active human NANOG protein can be utilized to elucidate the biological function of NANOG in various cellular processes associated with cancer and induced pluripotent stem cells.

## References

1. Booth HAF, Holland PWH (2004) Eleven daughters of NANOG. *Genomics* 84(2):229–238. <https://doi.org/10.1016/j.ygeno.2004.02.014>
2. Theunissen TW, Costa Y, Radziszewska A, van Oosten AL, Laval F, Pain B et al (2011) Reprogramming capacity of Nanog is functionally conserved in vertebrates and resides in a unique homeodomain. *Development* 138(22):4853–4865. <https://doi.org/10.1242/dev.068775>
3. Chambers I, Colby D, Robertson M, Nichols J, Lee S, Tweedie S, Smith A (2003) Functional expression cloning of Nanog, a pluripotency sustaining factor in embryonic stem cells. *Cell* 113(5):643–655. [https://doi.org/10.1016/S0092-8674\(03\)00392-1](https://doi.org/10.1016/S0092-8674(03)00392-1)
4. Mitsui K, Tokuzawa Y, Itoh H, Segawa K, Murakami M, Takahashi K et al (2003) The homeo-protein nanog is required for maintenance of pluripotency in mouse epiblast and ES cells. *Cell* 113(5):631–642. [https://doi.org/10.1016/S0092-8674\(03\)00393-3](https://doi.org/10.1016/S0092-8674(03)00393-3)
5. Komatsu K, Fujimori T (2015) Multiple phases in regulation of Nanog expression during pre-implantation development. *Dev Growth Differ* 57(9):648–656. <https://doi.org/10.1111/dgd.12244>
6. Chambers I, Silva J, Colby D, Nichol J, Nijmeijer B, Robertson M et al (2007) Nanog safeguards pluripotency and mediates germline development. *Nature* 450(7173):1230–1234. <https://doi.org/10.1038/nature06403>
7. Yamaguchi S, Kimura H, Tada M, Nakatsuji N, Tada T (2005) Nanog expression in mouse germ cell development. *Gene Expr Patterns* 5(5):639–646. <https://doi.org/10.1016/j.modgep.2005.03.001>
8. Laval F, Acloque H, Bertocchini F, MacLeod DJ, Boast S, Bachelard E et al (2007) The Oct4 homologue PouV and Nanog regulate pluripotency in chicken embryonic stem cells. *Development* 134(19):3549–3563. <https://doi.org/10.1242/dev.006569>
9. Silva J, Nichols J, Theunissen TW, Guo G, van Oosten AL, Barrandon O et al (2009) Nanog is the gateway to the pluripotent ground state. *Cell* 138(4):722–737. <https://doi.org/10.1016/j.cell.2009.07.039>



10. Messerschmidt DM, Kemler R (2010) Nanog is required for primitive endoderm formation through a non-cell autonomous mechanism. *Dev Biol* 344(1):129–137. <https://doi.org/10.1016/j.ydbio.2010.04.020>
11. Boyer LA, Lee TI, Cole MF, Johnstone SE, Levine SS, Zucker JP et al (2005) Core transcriptional regulatory circuitry in human embryonic stem cells. *Cell* 122(6):947–956. <https://doi.org/10.1016/j.cell.2005.08.020>
12. Loh YH, Wu Q, Chew JL, Vega VB, Zhang W, Chen X et al (2006) The Oct4 and Nanog transcription network regulates pluripotency in mouse embryonic stem cells. *Nat Genet* 38(4):431–440. <https://doi.org/10.1038/ng1760>
13. Wang J, Rao S, Chu J, Shen X, Levasseur DN, Theunissen TW, Orkin SH (2006) A protein interaction network for pluripotency of embryonic stem cells. *Nature* 444(7117):364–368. <https://doi.org/10.1038/nature05284>
14. Silva J, Chambers I, Pollard S, Smith A (2006) Nanog promotes transfer of pluripotency after cell fusion. *Nature* 441(7096):997–1001. <https://doi.org/10.1038/nature04914>
15. Hanna J, Saha K, Pando B, Van Zon J, Lengner CJ, Creighton MP et al (2009) Direct cell reprogramming is a stochastic process amenable to acceleration. *Nature* 462(7273):595–601. <https://doi.org/10.1038/nature08592>
16. Gingold JA, Fidalgo M, Guallar D, Lau Z, Sun Z, Zhou H et al (2014) A genome-wide RNAi screen identifies opposing functions of *snai1* and *snai2* on the nanog dependency in reprogramming. *Mol Cell* 56(1):140–152. <https://doi.org/10.1016/j.molcel.2014.08.014>
17. Theunissen TW, Van Oosten AL, Castelo-Branco G, Hall J, Smith A, Silva JCR (2011) Nanog overcomes reprogramming barriers and induces pluripotency in minimal conditions. *Curr Biol* 21(1):65–71. <https://doi.org/10.1016/j.cub.2010.11.074>
18. Zhao Y, Yin X, Qin H, Zhu F, Liu H, Yang Wet al (2008) Two supporting factors greatly improve the efficiency of human iPSC generation. *Cell Stem Cell* 3(5):475–479. <https://doi.org/10.1016/j.stem.2008.10.002>
19. Schwarz BA, Bar-Nur O, Silva JCR, Hochedlinger K (2014) Nanog is dispensable for the generation of induced pluripotent stem cells. *Curr Biol* 24(3):347–350. <https://doi.org/10.1016/j.cub.2013.12.050>
20. Carter AC, Davis-Dusenbery BN, Koszka K, Ichida JK, Eggan K (2014) Nanog-independent reprogramming to iPSCs with canonical factors. *Stem Cell Rep* 2(2):119–126. <https://doi.org/10.1016/j.stemcr.2013.12.010>
21. Yu J, Vodyanik MA, Smuga-Otto K, Antosiewicz-Bourget J, Frane JL, Tian S et al (2007) Induced pluripotent stem cell lines derived from human somatic cells. *Science* 318(5858):1917–1920. <https://doi.org/10.1126/science.1151526>
22. Maherali N, Ahfeldt T, Rigamonti A, Utikal J, Cowan C, Hochedlinger K (2008) A high-efficiency system for the generation and study of human induced pluripotent stem cells. *Cell Stem Cell* 3(3):340–345. <https://doi.org/10.1016/j.stem.2008.08.003>
23. Haase A, Olmer R, Schwanke K, Wunderlich S, Merkert S, Hess C et al (2009) Generation of induced pluripotent stem cells from human cord blood. *Cell Stem Cell* 5(4):434–441. <https://doi.org/10.1016/j.stem.2009.08.021>
24. Li Y, Zhao H, Lan F, Lee A, Chen L, Lin C et al (2010) Generation of human-induced pluripotent stem cells from gut mesentery-derived cells by ectopic expression of OCT4/SOX2/NANOG. *Cell Reprogramming (Formerly "Cloning and Stem Cells")*, 12(3):237–247. <https://doi.org/10.1089/cell.2009.0103>
25. Lowry WE, Richter L, Yachechko R, Pyle AD, Tchieu J, Sridharan R et al (2008) Generation of human induced pluripotent stem cells from dermal fibroblasts. *Proc Natl Acad Sci* 105(8):2883–2888. <https://doi.org/10.1073/pnas.0711983105>
26. Moon J-H, Yun W, Kim J, Hyeon S, Kang PJ, Park G et al (2013) Reprogramming of mouse fibroblasts into induced pluripotent stem cells with Nanog. *Biochem Biophys Res Commun* 431(3):444–449. <https://doi.org/10.1016/j.bbrc.2012.12.149>
27. Borgohain MP, Haridhasapavalan KK, Dey C, Adhikari P, Thummer RP (2019) An insight into DNA-free reprogramming approaches to generate integration-free induced pluripotent stem cells for prospective biomedical applications. *Stem Cell Rev Rep* 15(2):286–313. <https://doi.org/10.1007/s12015-018-9861-6>

28. Haridhasapavalan KK, Borgohain MP, Dey C, Saha B, Narayan G, Kumar S, Thummer RP (2019) An insight into non-integrative gene delivery approaches to generate transgene-free induced pluripotent stem cells. *Gene* 686:146–159. <https://doi.org/10.1016/j.gene.2018.11.069>
29. Dey C, Raina K, Haridhasapavalan KK, Thool M, Sundaravadivelu PK, Adhikari P et al (2021) An overview of reprogramming approaches to derive integration-free induced pluripotent stem cells for prospective biomedical applications. *Recent Adv iPSC Technol* 231–287. <https://doi.org/10.1016/B978-0-12-822231-7.00011-4>
30. Fishedick G, Wu G, Adachi K, Araúzo-Bravo MJ, Greber B, Radstaak M et al (2014) Nanog induces hyperplasia without initiating tumors. *Stem Cell Res* 13(2):300–315. <https://doi.org/10.1016/j.scr.2014.08.001>
31. Ezeh UI, Turek PJ, Reijo RA, Clark AT (2005) Human embryonic stem cell genes OCT4, NANOG, STELLAR, and GDF3 are expressed in both seminoma and breast carcinoma. *Cancer: Interdiscip Int J Am Cancer Soc* 104(10):2255–2265. <https://doi.org/10.1002/cncr.21432>
32. Bussolati B, Bruno S, Grange C, Ferrando U, Camussi G (2008) Identification of a tumor-initiating stem cell population in human renal carcinomas. *FASEB J* 22(10):3696–3705. <https://doi.org/10.1096/fj.08-102590>
33. Ye F, Zhou C, Cheng Q, Shen J, Chen H (2008) Stem-cell-abundant proteins Nanog, Nucleostemin and Musashi 1 are highly expressed in malignant cervical epithelial cells. *BMC Cancer* 8(1):1–5. <https://doi.org/10.1186/1471-2407-8-108>
34. Thool M, Dey C, Bhattacharyya S, Sudhagar S, Thummer RP (2021) Generation of a recombinant stem cell-specific human SOX2 protein from *Escherichia coli* under native conditions. *Mol Biotechnol* 63(4):327–338. <https://doi.org/10.1007/s12033-021-00305-y>
35. Haridhasapavalan KK, Sundaravadivelu PK, Bhattacharyya S, Ranjan SH, Raina K, Thummer RP (2021) Generation of cell-permeant recombinant human transcription factor GATA4 from *E. coli*. *Bioprocess Biosyst Eng* 44(6):1131–1146. <https://doi.org/10.1007/s00449-021-02516-8>
36. Bradford MM (1976) A rapid and sensitive method for the quantitation of microgram quantities of protein utilizing the principle of protein-dye binding. *Anal Biochem* 72(1–2):248–254. <https://doi.org/10.1006/abio.1976.9999>
37. Micsonai A, Wien F, Bulyáki É, Kun J, Moussong É, Lee Y-H et al (2018) BeStSel: a web server for accurate protein secondary structure prediction and fold recognition from the circular dichroism spectra. *Nucleic Acids Res* 46(W1):W315–W322. <https://doi.org/10.1093/nar/gky497>
38. Micsonai A, Bulyáki É, Kardos J (2021) BeStSel: from secondary structure analysis to protein fold prediction by circular dichroism spectroscopy. In: *Structural genomics*. Springer, Berlin, pp 175–189. [https://doi.org/10.1007/978-1-0716-0892-0\\_11](https://doi.org/10.1007/978-1-0716-0892-0_11)
39. Dey C, Thool M, Bhattacharyya S, Sudhagar S, Thummer RP (2021) Generation of biologically active recombinant human OCT4 protein from *E. coli*. *3 Biotech* 11(5):1–16. <https://doi.org/10.1007/s13205-021-02758-z>
40. Narayan G, Agrawal A, Joshi N, Gogoi R, Nagotu S, Thummer RP (2021) Protein production and purification of a codon-optimized human NGN3 transcription factor from *E. coli*. *Protein J* 40(6):891–906. <https://doi.org/10.1007/s10930-021-10020-x>
41. Patel TB, Bertics PJ (2006) *Epidermal growth factor: methods and protocols*, vol 327. Springer Science & Business Media
42. Dey C, Venkatesan V, Thummer RP (2022) Identification of optimal expression parameters and purification of a codon-optimized human GLIS1 transcription factor from *Escherichia coli*. *Mol Biotechnol* 64(1):42–56. <https://doi.org/10.1007/s12033-021-00390-z>
43. Grada A, Otero-Vinas M, Prieto-Castrillo F, Obagi Z, Falanga V (2017) Research techniques made simple: analysis of collective cell migration using the wound healing assay. *J Investig Dermatol* 137(2):e11–e16. <https://doi.org/10.1016/j.jid.2016.11.020>
44. Haridhasapavalan KK, Das NJ, Thummer RP (2022) Generation of a transducible version of a bioactive recombinant human TBX5 transcription factor from *E. Coli*. *Curr Res Biotechnol* 4:66–77
45. Jauch R, Ng CKL, Saikatendu KS, Stevens RC, Kolatkar PR (2008) Crystal structure and DNA binding of the homeodomain of the stem cell transcription factor Nanog. *J Mol Biol* 376(3):758–770. <https://doi.org/10.1016/j.jmb.2007.11.091>

46. Hu PF, Guan WJ, Li XC, Ma YH (2012) Construction of recombinant proteins for reprogramming of endangered Luxi cattle fibroblast cells. *Mol Biol Rep* 39(6):7175–7182. <https://doi.org/10.1007/s11033-012-1549-4>
47. Yu M, Lian S, Han H, Yu K, Li G, Lian Z, Li N (2013) Four recombinant pluripotency transcriptional factors containing a protein transduction domain maintained the in vitro pluripotency of chicken embryonic stem cells. *Sci China Life Sci* 56(1):40–50. <https://doi.org/10.1007/s11427-012-4426-4>
48. Zhang H, Ma Y, Gu J, Liao B, Li J, Wong J, Jin Y (2012) Reprogramming of somatic cells via TAT-mediated protein transduction of recombinant factors. *Biomaterials* 33(20):5047–5055. <https://doi.org/10.1016/j.biomaterials.2012.03.061>
49. Yang WC, Patel KG, Lee J, Ghebremariam YT, Wong HE, Cooke JP, Swartz JR (2009) Cell-free production of transducible transcription factors for nuclear reprogramming. *Biotechnol Bioeng* 104(6):1047–1058. <https://doi.org/10.1002/bit.22517>
50. Yang WC, Welsh JP, Lee J, Cooke JP, Swartz JR (2011) Solubility partner IF2 Domain I enables high yield synthesis of transducible transcription factors in *Escherichia coli*. *Protein Expr Purif* 80(1):145–151. <https://doi.org/10.1016/j.pep.2011.06.017>
51. Ha SC, Pereira JH, Jeong JH, Huh JH, Kim SH (2009) Purification of human transcription factors Nanog and Sox2, each in complex with Skp, an *Escherichia coli* periplasmic chaperone. *Protein Expr Purif* 67(2):164–168. <https://doi.org/10.1016/j.pep.2009.05.003>
52. Kelly SM, Jess TJ, Price NC (2005) How to study proteins by circular dichroism. *Biochimica et Biophysica Acta (BBA)-Proteins and Proteomics*, 1751(2):119–139. <https://doi.org/10.1016/j.bbapap.2005.06.005>
53. Micsonai A, Wien F, Kernya L, Lee Y-H, Goto Y, Réfrégiers M, Kardos J (2015) Accurate secondary structure prediction and fold recognition for circular dichroism spectroscopy. *Proc Natl Acad Sci* 112(24):E3095–E3103. <https://doi.org/10.1073/pnas.1500851112>
54. Yu Z, Huang Z, Lung ML (2013) Subcellular fractionation of cultured human cell lines. *Bio-Protoc* 3(9):e754–e754
55. Do HJ, Lim HY, Kim JH, Song H, Chung HM, Kim JH (2007) An intact homeobox domain is required for complete nuclear localization of human Nanog. *Biochem Biophys Res Commun* 353(3):770–775. <https://doi.org/10.1016/j.bbrc.2006.12.100>
56. Chang DF, Tsai SC, Wang XC, Xia P, Senadheera D, Lutzko C (2009) Molecular characterization of the human NANOG protein. *Stem Cells* 27(4):812–821. <https://doi.org/10.1634/stemcells.2008-0657>
57. Zhang J, Wang X, Chen B, Suo G, Zhao Y, Duan Z, Dai J (2005) Expression of Nanog gene promotes NIH3T3 cell proliferation. *Biochem Biophys Res Commun* 338(2):1098–1102. <https://doi.org/10.1016/j.bbrc.2005.10.071>
58. Peitz M, Müntz B, Thummer RP, Helfen M, Edenhofer F (2014) Cell-permeant recombinant Nanog protein promotes pluripotency by inhibiting endodermal specification. *Stem Cell Res* 12(3):680–689. <https://doi.org/10.1016/j.scr.2014.02.006>
59. Gu TT, Liu SY, Zheng PS (2012) Cytoplasmic NANOG-positive stromal cells promote human cervical cancer progression. *Am J Pathol* 181(2):652–661. <https://doi.org/10.1016/j.ajpath.2012.04.008>
60. Ding Y, Yu AQ, Li CL, Fang J, Zeng Y, Li DS (2014) TALEN-mediated Nanog disruption results in less invasiveness, more chemosensitivity and reversal of EMT in HeLa cells. *Oncotarget* 5(18):8393–8401. <https://doi.org/10.18632/oncotarget.2298>
61. Ding Y, Yu AQ, Wang XL, Guo XR, Yuan YH, Li DS (2016) Forced expression of Nanog with mRNA synthesized in vitro to evaluate the malignancy of HeLa cells through acquiring cancer stem cell phenotypes. *Oncol Rep* 35(5):2643–2650. <https://doi.org/10.3892/or.2016.4639>
62. Müntz B, Thier MC, Winnemöller D, Helfen M, Thummer RP, Edenhofer F (2016) Nanog induces suppression of senescence through downregulation of p27KIP1 expression. *J Cell Sci* 129(5):912–920. <https://doi.org/10.1242/jcs.167932>
63. Oh JH, Do HJ, Yang HM, Moon SY, Cha KY, Chung HM, Kim JH (2005) Identification of a putative transactivation domain in human Nanog. *Exp Mol Med* 37(3):250–254. <https://doi.org/10.1038/emmm.2005.33>

64. Jeter CR, Yang T, Wang J, Chao HP, Tang DG (2015) Concise review: NANOG in cancer stem cells and tumor development: an update and outstanding questions. *Stem Cells* 33(8):2381–2390. <https://doi.org/10.1002/stem.2007>
65. Patra SK, Vemulawada C, Soren MM, Sundaray JK, Panda MK, Barman HK (2018) Molecular characterization and expression patterns of Nanog gene validating its involvement in the embryonic development and maintenance of spermatogonial stem cells of farmed carp, *Labeo rohita*. *J Anim Sci Biotechnol* 9(1):1–17. <https://doi.org/10.1186/s40104-018-0260-2>
66. Stuart HT, Van Oosten AL, Radziszewska A, Martello G, Miller A, Dietmann S et al (2014) NANOG amplifies STAT3 activation and they synergistically induce the naive pluripotent program. *Curr Biol* 24(3):340–346. <https://doi.org/10.1016/j.cub.2013.12.040>
67. Choi KJ, Quan MD, Qi C, Lee JH, Tsoi PS, Zahabiyon M et al (2022) NANOG prion-like assembly mediates DNA bridging to facilitate chromatin reorganization and activation of pluripotency. *Nature Cell Biol* 24(5):737–747. <https://doi.org/10.1038/s41556-022-00896-x>
68. Bothmann H, Plückthun A (1998) Selection for a periplasmic factor improving phage display and functional periplasmic expression. *Nat Biotechnol* 16(4):376–380. <https://doi.org/10.1038/nbt0498-376>
69. Hayashi Y, Caboni L, Das D, Yumoto F, Clayton T, Deller MC et al (2015) Structure-based discovery of NANOG variant with enhanced properties to promote self-renewal and reprogramming of pluripotent stem cells. *Proc Natl Acad Sci U S A* 112(15):4666–4671. <https://doi.org/10.1073/pnas.1502855112>
70. Bosnali M, Edenhofer F (2008) Generation of transducible versions of transcription factors Oct4 and Sox2. *Biol Chem* 389(7):851–861. <https://doi.org/10.1515/BC.2008.106>
71. Stock K, Nolden L, Edenhofer F, Quandt T, Brüstle O (2010) Transcription factor-based modulation of neural stem cell differentiation using direct protein transduction. *Cell Mol Life Sci* 67(14):2439–2449. <https://doi.org/10.1007/s00018-010-0347-1>
72. Thier M, Müntz B, Edenhofer F (2011) Exploring refined conditions for reprogramming cells by recombinant Oct4 protein. *Int J Dev Biol* 54(11–12):1713–1721. <https://doi.org/10.1387/ijdb.103193mt>
73. Thier M, Müntz B, Mielke S, Edenhofer F (2012) Cellular reprogramming employing recombinant Sox2 protein. *Stem Cells Int*. <https://doi.org/10.1155/2012/549846>
74. Narayan G, Sundaravadivelu PK, Agrawal A, Gogoi R, Nagotu S, Thummer RP (2021) Soluble expression, purification, and secondary structure determination of human PDX1 transcription factor. *Protein Expr Purif* 180:105807. <https://doi.org/10.1016/j.pep.2020.105807>
75. Haridhasapavalan KK, Sundaravadivelu PK, Voorkara U, Kaveeshwar V, Thummer RP (2022) Generation of the recombinant version of a bioactive human MEF2C transcription factor from *E. coli*. In: *Healthcare research and related technologies-proceedings of NERC*. Springer Nature
76. Haridhasapavalan KK, Sundaravadivelu PK, Thummer RP (2020) Codon optimization, cloning, expression, purification, and secondary structure determination of human ETS2 transcription factor. *Mol Biotechnol* 62(10):485–494. <https://doi.org/10.1007/s12033-020-00266-8>
77. Haridhasapavalan KK, Ranjan SH, Bhattacharyya S, Thummer RP (2021) Soluble expression, purification, and secondary structure determination of human MESP1 transcription factor. *Appl Microbiol Biotechnol* 105(6):2363–2376. <https://doi.org/10.1007/s00253-021-11194-1>
78. Haridhasapavalan KK, Sundaravadivelu PK, Joshi N, Das NJ, Mohapatra A, Voorkara U et al (2022) Generation of a recombinant version of a biologically active cell-permeant human HAND2 transcription factor from *E. coli*. *Sci Rep* 12(1):16129. <https://doi.org/10.1038/s41598-022-19745-w>